

**AIR SURFACE TEMPERATURE CORRELATION
WITH GREENHOUSE GASES USING AIRS DATA
OVER PENINSULAR MALAYSIA**

by

JASIM MOHAMMED RAJAB HUSSAIN

**Thesis submitted in fulfillment of the requirements for the
degree of
Doctor of Philosophy**

August 2011

ACKNOWLEDGEMENTS

In the name of Allah, Most Gracious, Most Merciful

First of all, I would like to thank Allah the Almighty for granting me health, patience and determination to complete this doctoral study. I would also like to thank my main and co. supervisors Associate Professor Dr. Mohad Zubir-Mat Jafri and Dr. Lim Hwee San for their supervision, guidance, time, moral support, scientific support and valuable questions from the early stages of this research.

I would like to express my gratitude to Dr. Abbas F. M. AL-Karkhi and Dr. Khalid M. Omar for their time, guidance and valuable academic consultation. A lot of thanks go to my great-uncle Dr. Salim Taib Yousif for his support, time and guidance. I would like to thank the Institute of Postgraduate Students of Universiti Sains Malaysia for a Postgraduate Research Grant (PRGS, Grant No. 1001/PFIZIK/841029) to finance the project. My appreciation goes to the AIRS staff for their generosity on sharing some valuable satellite data with public.

I would like to thank those who were and will remain just like my soul, my great and marvelous father, true love mother, family, lovely darling daughters, and supporting brothers and sisters. Without the constant support and encouragement from all of them, it would have been impossible to accomplish this study. I am indebted to my siblings, relatives, and friends for their continuous prayers and moral support.

Eventually, I would like to express my gratitude to all my lab mates, staff, friends and colleagues who supported me and helped me at the School of Physics / Universiti Sains Malaysia.



TABLE OF CONTENTS

| | Page |
|---|------|
| ACKNOWLEDGEMENTS | ii |
| TABLE OF CONTENTS | iii |
| LIST OF TABLES | vi |
| LIST OF FIGURES | vii |
| LIST OF SYMBOLS | x |
| LIST OF ABBREVIATION | xi |
| ABSTRAK | xiii |
| ABSTRACT | xv |
| | |
| CHAPTER 1: INTRODUCTION | |
| 1.0 Overview | 1 |
| 1.1 Greenhouse gases (GHGs) | 4 |
| 1.1.1 Water Vapour (H_2O_{vapour}) | 5 |
| 1.1.2 Carbon Dioxide (CO_2) | 6 |
| 1.1.3 Ozone (O_3) | 6 |
| 1.1.4 Methane (CH_4) | 7 |
| 1.1.5 Carbon Monoxide (CO) | 8 |
| 1.2 IPCC and Global Warming | 9 |
| 1.3 A Definition and Brief History of Remote Sensing | 12 |
| 1.4 Remote Sensing Space Platforms | 14 |
| 1.5 Problem statement | 16 |
| 1.6 Objectives of the study | 17 |
| 1.7 Originality | 18 |
| 1.8 Outline of the thesis | 18 |
| | |
| CHAPTER 2: LITERATURE REVIEW | |
| 2.0 Introduction | 20 |
| 2.1 Greenhouse gases and temperature in Malaysia | 21 |
| 2.2 Atmospheric composition—minor gases from AIRS | 23 |
| 2.3 Statistical methods and regression analysis | 29 |
| 2.4 Summary | 31 |
| | |
| CHAPTER 3: INTRODUCTION TO AIRS, DATA AND SOFTWARE | |
| 3.1 The AIRS and AMSU specifications | 32 |
| 3.2 AIRS Instrument Description | 34 |
| 3.2.1 Atmospheric Infrared Sounder (AIRS) | 34 |
| 3.2.2 Advanced Microwave Sounding Unit (AMSU-A) | 35 |
| 3.3 AIRS Science Processing System - Level-3 Processing | 36 |
| 3.4 AIRS mid-Troposphere CO_2 Products | 37 |
| 3.5 AIRS Science Objectives | 38 |

| | | |
|--|---|-----|
| 3.6 | Remotely Sensed Data | 40 |
| 3.7 | The AIRS / AMSU Standard data | 41 |
| 3.8 | Sources of Data | 43 |
| 3.8.1 | Satellite data | 43 |
| 3.8.2 | <i>In situ</i> data | 44 |
| 3.9 | Software and Tools | 44 |
| | | |
| CHAPTER 4: GENERATING THE REGRESSION MODELS | | |
| 4.0 | Introduction | 47 |
| 4.1 | Study Area | 47 |
| 4.2 | Methodology | 49 |
| 4.2.1 | Regression | 50 |
| 4.2.2 | Multiple Regression Analysis (MRA) | 51 |
| 4.2.3 | Principal Component Analysis (PCA) | 52 |
| 4.3 | Procedures | 54 |
| | | |
| CHAPTER 5: RESULTS AND DISCUSSION | | |
| 5.0 | Introduction | 59 |
| 5.1 | Multiple regression analysis of air surface temperature [AST] | 59 |
| 5.1.1 | Generating regression equation AST1 using standard AIRX3STM data | 60 |
| 5.1.1.1 | Regression analysis of the impact of GHGs on AST1 | 61 |
| 5.1.2 | Generating regression equation AST2 using Standard AIRX3STM and AIRX3C2M data | 68 |
| 5.1.2.1 | Regression analyses of the impact of GHGs on AST2 | 69 |
| 5.2 | Generating regression equations for O ₃ using standard AIRX3STM product data | 73 |
| 5.2.1 | Analysis of ozone data | 73 |
| 5.2.2 | Principle component analysis (PCA) | 75 |
| 5.2.3 | Model fitting | 77 |
| 5.3 | Evaluation of atmospheric gas values from AIRS observation data | 77 |
| 5.4 | Mapping | 86 |
| 5.4.1 | Carbon dioxide | 87 |
| 5.4.2 | Methane | 91 |
| 5.4.3 | Carbon monoxide | 94 |
| | | |
| CHAPTER 6: COMPARISON AND VALIDATION OF THE REGRESSION MODELS | | |
| 6.0 | Introduction | 98 |
| 6.1 | Comparison of AST | 99 |
| 6.1.1 | Comparison of AST1 and AST2 with observed AST from AIRS and <i>in situ</i> measurement. | 99 |
| 6.1.2 | Direct comparison of AST1 and AST2 with observed AST from AIRS using mapping | 103 |
| 6.2 | Validation | 105 |

| | |
|--|-----|
| 6.2.1 Validation of the AST | 105 |
| 6.2.1.1 Validation of AST1 and AST2 with observed AST from AIRS | 106 |
| 6.2.2 Validation of the principal component analysis (PCA) | 110 |
| 6.2.2.1 Validation of the predicted O ₃ with the observed AIRS O ₃ | 110 |
| 6.3 AST1 distribution over the study area for 2009 | 113 |
| 6.4 Ozone distribution from the predicted algorithms over the study area in 2009 | 119 |
| | |
| CHAPTER 7: CONCLUSIONS AND FUTURE WORK | |
| 7.1 Conclusions | 122 |
| 7.2 Suggestions for future work | 126 |
| | |
| REFERENCES | 128 |
| | |
| APPENDIXES | |
| Appendix A: Level 3 Standard Product Interface Specification | 139 |
| Appendix B: The List of channels by function that are used in the Version 5 retrieval | 144 |
| Appendix C: The <i>in situ</i> air surface temperature (AST) data for all stations | 146 |
| Appendix D: The correlation for all months from January 2003 to December 2008 | 148 |
| Appendix E: The monthly rainfall amount from January 2003 to December 2009 for five stations {Unit: millimeter (mm)} | 148 |
| | |
| LIST OF PUBLICATIONS | 150 |

LIST OF TABLES

| | | Page |
|-----------|---|------|
| Table 3.1 | AIRS Technology-Specifications | 34 |
| Table 3.2 | AMSU instrument characteristics | 35 |
| Table 3.3 | Level-1, Level-2 and Level-3 data set products | 37 |
| Table 3.4 | Level-2 and Level-3 CO ₂ data set products | 38 |
| Table 5.1 | The estimated regression coefficient B for AIRX3STM data | 61 |
| Table 5.2 | The estimated regression coefficient β for AIRX3STM data | 62 |
| Table 5.3 | The estimated regression coefficient B for AIRX3STM and AIRX3C2M data | 69 |
| Table 5.4 | The estimated regression coefficient β for AIRX3STM and AIRX3C2M data | 70 |
| Table 5.5 | Pearson correlation matrix of different variables for NEM and SWM season | 74 |
| Table 5.6 | Rotated principal components loadings for NEM and SWM season | 75 |
| Table 5.7 | Linear regression model for prediction of O ₃ using the principle components | 76 |

LIST OF FIGURES

| | | Page |
|------------|---|------|
| Figure 1.1 | From IPCC 4th Assessment Report, (a) Global annual emissions of anthropogenic GHGs from 1970 to 2004. (b) Share of different anthropogenic GHGs in total emissions in 2004. (c) Share of different sectors in total anthropogenic GHG emissions in 2004. | 11 |
| Figure 1.2 | Global-average radiative forcing (RF) in 2005 (best estimates and 5-95% uncertainty ranges) with respect to 1750 for CO ₂ , CH ₄ , N ₂ O and other important agents and mechanisms, together with the typical geographical extent (spatial scale) of the forcing and the assessed level of scientific understanding (LOSU). Aerosols from explosive volcanic eruptions contribute an additional episodic cooling term for a few years following an eruption. | 11 |
| Figure 1.3 | Observed changes in (a) global average surface temperature; (b) global average sea level from tide gauge (blue) and satellite (red) data and (c) Northern Hemisphere snow cover for March-April. All differences are relative to corresponding averages for the period 1961-1990. Smoothed curves represent decadal averaged values while circles show yearly values. The shaded areas are the uncertainty intervals estimated from a comprehensive analysis of known uncertainties (a and b) and from the time series (c). | 12 |
| Figure 3.1 | Schematic showing the AIRS and AMSU scan geometries | 33 |
| Figure 3.2 | The AIRS monthly Level-3 Standard products at 28 levels | 42 |
| Figure 4.1 | The geographical feature of the study area | 48 |
| Figure 4.2 | Flow chart of methodology applied in this research. | 58 |
| Figure 5.1 | Monthly ground air temperature, rainfall, carbon monoxide, total column ozone, methane, and troposphere carbon dioxide between January 2003 and December 2009 for Subang site. | 81 |
| Figure 5.2 | Monthly ground air temperature, rainfall, carbon monoxide, total column ozone, methane, and troposphere carbon dioxide between January 2003 and December 2009 for Penang site. | 82 |
| Figure 5.3 | Monthly ground air temperature, rainfall, carbon monoxide, total column ozone, methane, and troposphere carbon dioxide between January 2003 and December 2009 for Kuantan site. | 83 |
| Figure 5.4 | Monthly ground air temperature, rainfall, carbon monoxide, total column ozone, methane, and troposphere carbon dioxide between January 2003 and December 2009 for Johor Bahru site. | 84 |

| | | |
|-------------|---|-----|
| Figure 5.5 | Monthly ground air temperature, rainfall, carbon monoxide, total column ozone, methane, and troposphere carbon dioxide between January 2003 and December 2009 for Kota Bahru site. | 85 |
| Figure 5.6 | AIRS monthly coverage for the retrieved mid-troposphere carbon dioxide (CO ₂) during the NEM season [November - April] of 2009. | 89 |
| Figure 5.7 | AIRS monthly coverage for the retrieved mid-troposphere carbon dioxide columns (CO ₂) during the SWM season [May - October] of 2009. | 90 |
| Figure 5.8 | AIRS monthly coverage from the retrieved effective volume mixing of methane (CH ₄) during the NEM season [November - April] of 2009. | 92 |
| Figure 5.9 | AIRS monthly coverage from the retrieved effective volume mixing of methane (CH ₄) during the SWM season [May - October] of 2009. | 93 |
| Figure 5.10 | AIRS monthly coverage from the retrieved total column carbon monoxide (CO) during the NEM season [November - April] of 2009. | 96 |
| Figure 5.11 | AIRS monthly coverage from retrieved total column carbon monoxide (CO) during the SWM season [May - October] of 2009. | 97 |
| Figure 6.1 | Observed AST from AIRS (solid line), <i>in situ</i> AST measurements (dotted line), and predicted AST1 (dashed line) in 2009 for the Kota Bahru, Penang, Kuantan, Subang, and Johor stations. | 101 |
| Figure 6.2 | Observed AST from AIRS (solid line), <i>in situ</i> AST measurements (dotted line), and predicted AST2 (dashed line) in 2009 for the Kota Bahru, Penang, Kuantan, Subang, and Johor stations. | 102 |
| Figure 6.3 | Peninsular Malaysia AIRS AST (Top), predicted AST1 (Middle), and differences (AIRS - predicted AST1) (Bottom), left for January and right for August, respectively, 2009. | 104 |
| Figure 6.4 | Peninsular Malaysia AIRS AST (Top), predicted AST2 (Middle), and differences (AIRS - predicted AST1) (Bottom), left for January and right for August, respectively, 2009. | 105 |
| Figure 6.5 | Predicted values of AST1 vs. the observed AST from AIRS for January and August 2009. | 107 |

| | | |
|-------------|---|-----|
| Figure 6.6 | Predicted values of AST1 vs. the observed AST from AIRS for the Kota Bahru, Penang, Kuantan, Subang, and Johor stations for 2009. | 108 |
| Figure 6.7 | Predicted values of AST2 vs. the observed AST from AIRS for the Kota Bahru, Penang, Kuantan, Subang, and Johor stations for 2009. | 109 |
| Figure 6.8 | Predicted values of AST2 vs. the observed AST from AIRS for January and August 2009. | 110 |
| Figure 6.9 | Predicted vs. observed values of O ₃ from AIRS for the months of December, January, July, and August, and at Subang station for 2009. | 111 |
| Figure 6.10 | Observed ozone from AIRS (solid line), <i>in situ</i> measurements (dotted line), and predicted value (dashed line) in 2009 for the Subang station. | 112 |
| Figure 6.11 | Monthly AST1 distribution over peninsular Malaysia from November–April, the NEM season, of 2009. | 115 |
| Figure 6.12 | Monthly AST1 distribution over peninsular Malaysia from May to October, the SWM season, of 2009. | 118 |
| Figure 6.13 | Monthly total column ozone (O ₃) for the NEM season (November–April) in 2009. | 120 |
| Figure 6.14 | Monthly total column ozone (O ₃) for the SWM season (May - October) in 2009. | 121 |

LIST OF SYMBOLS

| | |
|------------------------------------|----------------------------|
| Ar | Argon |
| CH ₄ | Methane |
| CO | Carbon Monoxide |
| CO ₂ | Carbon Dioxide |
| F _c | CO ₂ flux |
| F _{storage} | CO ₂ storage |
| H | Hydrogen |
| H ₂ O _{vapour} | Water vapour |
| N ₂ | Nitrogen |
| N ₂ O | Nitric Acid |
| NO ₂ | Nitrogen Dioxide |
| NO _x | Nitrogen oxides |
| O ₂ | Oxygen |
| O ₃ | Ozone |
| OH | Hydroxyl radicals |
| VOCs | Volatilé Organic Compounds |

LIST OF ABBREVIATION

| | |
|----------|---|
| AERI | Atmospheric Emitted Radiance Interferometer |
| AIRS | Atmospheric InfraRed Sounder |
| AMSR-E | Advanced Microwave Scanning Radiometer |
| AMSU | Advanced Microwave Sounding Unit |
| ANN | Artificial Neural Network |
| APT | Automatic Picture Transmission |
| ASO | August-September-October |
| AST | Air surface temperature |
| AT | Atmospheric Temperature |
| DB | Direct Broadcast |
| DN | Data Numbers |
| DOE | Department Of Environment |
| DTR | Diurnal temperature range |
| DU | Dobson Unit |
| ECMWF | European Center for Medium-range Weather Forecast |
| EDOS | Earth Data and Operations System |
| EOS | Earth Observing System |
| ERTS | Earth Resources Technology Satellite |
| EU | Engineering Units |
| FMA | February-March-April |
| GHGs | Greenhouse gases |
| Gt C/y | Giga tons carbon per year |
| HDF | Hierarchical Data Format |
| HDF-EOS | Hierarchical Data Format-Earth Observing System |
| HIRDLS | High Resolution Dynamics Limb Sounder |
| HSB | Humidity Sounder for Brazil |
| IASI | Infrared Atmospheric Sounding Interferometer |
| IOD | Indian Ocean Dipole |
| IPCC | Intergovernmental Panel on Climate Change |
| IR | Infrared |
| IR/MW | Infrared/Microwave |
| L1 | Level-1 |
| L2 | Level-2 |
| L3 | Level-3 |
| MJJ | May-June-July |
| MLS | Microwave Limb Sounder |
| MMD | Malaysian Meteorological Department |
| MOPITT | Measurements of Pollution in the Troposphere |
| MR | Multiple Regressions |
| MRA | Multiple Regression Analysis |
| MS-Excel | Microsoft Excel |

| | |
|-----------|--|
| MSP | Mean Surface Pressure |
| Mt | Megatons |
| MW | Microwave |
| MW-Only | Microwave-Only |
| NDJ | November-December-January |
| NEE | Net Ecosystem Exchange |
| NEM | Northeast Monsoon |
| NH | Northern Hemisphere |
| NOAA | National Oceanic and Atmospheric Administration |
| NASA | National Aeronautics and Space Administration |
| OMI | Ozone Monitoring Instrument |
| PCs | Principal Components |
| PCA | Principal Component Analysis |
| PGEs | Product Generation Executives |
| PM | Particulate Matter |
| PV | Potential Vorticity |
| PWV | Perceptible Water Vapour |
| QA | Quality Assessment |
| RH | Relative Humidity |
| RMS | Root Mean Square |
| RMSE | Root Mean Square Errors |
| RG SST | Real Global Sea Surface Temperature |
| SCIAMACHY | Scanning Imaging Absorption Spectrometer for Atmospheric Cartography |
| SMS | Synchronous Meteorological Satellite |
| SPS | Science Processing System |
| SPSS | Statistical Package for Social Sciences |
| SST | Sea Surface Temperature |
| SSKT | Surface Skin Temperature |
| START08 | Stratosphere-Troposphere Analysis of Regional Transport 2008 |
| SWM | Southwest Monsoon |
| sza | satellite zenith angle |
| TDOGW | The Discovery of Global Warming |
| TIROS | Television Infra Red Observation Satellite |
| TM3 | Tracer Model version 3 |
| TOA | Top of the atmosphere |
| UTLS | Upper Troposphere and Lower Stratosphere |
| UTWV | Upper Tropospheric Water Vapour |
| UV | Ultraviolet |
| (UV)-B | Biological harmful ultraviolet |
| VIS | Visible |

KORELASI SUHU PERMUKAAN UDARA DENGAN GAS RUMAH HIJAU MENGGUNAKAN DATA AIRS DI SEMENANJUNG MALAYSIA.

ABSTRAK

Objektif utama kajian ini adalah untuk membangunkan empat persamaan regresi AST1, AST2, PCA1 (Analisis komponen utama) (O_3 musim NEM (monsun timur laut)), dan PCA2 (O_3 musim SWM (monsun barat daya)) untuk mengira suhu permukaan udara AST dan O_3 . Di samping itu, kajian ini turut menganalisis serta mengkaji impak GHGs (gas rumah hijau) terhadap nilai AST dan beberapa parameter atmosfera pada nilai O_3 di Semenanjung Malaysia. Kaedah linear pelbagai dan regresi komponen utama digunakan untuk mencapai objektif kajian.

AST1 ($R= 0.821$) dan AST2 ($R= 0.783$) yang diramal didapati mempunyai korelasi yang amat tinggi dengan gas rumah hijau untuk data selama enam-tahun (2003–2008). Perbandingan dalam kalangan lima stesen pada tahun 2009 menunjukkan terdapat kesamaan di antara AST1 dan AST2 yang diramal dan AST yang dicerap daripada AIRS, terutama ketika musim SWM, sekitar 1.3 K, dan untuk data *in situ*, sekitar 1 hingga 2 K. Keputusan pengesahan kedua-dua AST1 dan AST2 yang berasaskan AST daripada AIRS menunjukkan perkali korelasi yang tinggi ($R= 0.845 - 0.918$) dan ($0.808 - 0.878$) masing-masing. Ini menjadi penunjuk kepada kecekapan dan ketepatan kedua-dua persamaan.

Analisis statistik dalam bentuk β menunjukkan bahawa H_2O_{wap} (0.565–1.746) cenderung untuk menyumbang secara signifikan terhadap nilai AST yang tinggi semasa musim NEW. H_2O_{wap} (1.042–2.036) dan O_3 semasa musim monsun SWM ditunjukkan melalui pekali β (0.421-0.864) yang amat positif. CO mempunyai pekali β (0.154–0.96) sederhana positif yang dikaitkan dengan nilai AST, dan CH_4 (-0.525–0.426) juga merupakan parameter penting dalam menentukan kebolehubahan nilai

AST. CO₂ menghasilkan suatu hubungan yang munasabah dengan AST melalui nilai pekali β , daripada yang rendah hingga sederhana (antara -0.065 hingga 0.238).

Keputusan penyesuaian persamaan regresi terbaik untuk data O₃, memberikan nilai pekali ($R \approx 0.93$) dan ($R^2 \approx 0.86$) yang hampir sama, bagi kedua-dua musim NEM dan SWM. Pemboleh ubah sepunya yang wujud dalam kedua-dua persamaan PCA1 dan PCA2 dengan SSKT (Suhu permukaan kulit), CH₄ dan RH, dan prekursor utama nilai O₃ bagi kedua-dua musim NEM dan SWM adalah SSKT. Pengesahan keputusan menunjukkan pekali korelasi yang tinggi (0.845–0.942), dan pekali yang dilaras (0.713–0.887) adalah bukti bagi keberkesanan persamaan regresi O₃.

Secara keseluruhan, keputusan ini dengan jelasnya menunjukkan kebaikan menggunakan data daripada satelit AIRS dan kajian analisis korelasi untuk mengkaji impak atmosfera GHGs pada AST di seluruh Semenanjung Malaysia. Persamaan regresi yang dibangunkan berupaya mengesan AST di Semenanjung Malaysia dalam semua keadaan cuaca dengan ketidaktentuan total berjulat di antara 1 hingga 2 K.

AIR SURFACE TEMPERATURE CORRELATION WITH GREENHOUSE GASES USING AIRS DATA OVER PENINSULAR MALAYSIA

ABSTRACT

The main objective of this study is to develop four regression equations—denoted AST1, AST2, PCA1 (O₃ NEM season), and PCA2 (O₃ SWM season)—that will then be used to calculate the air surface temperature (AST) and total column ozone (O₃). In addition, this study seeks to analyse and investigate the impacts of greenhouse gases (GHGs) on the AST value and several atmospheric parameters on O₃ values in Peninsular Malaysia. Multiple linear and principal component regression methods have been used to achieve the objectives of the study.

The predicted AST1 (R= 0.821) and AST2 (R= 0.783) were highly correlated with GHGs for the six-year (2003–2008) data. Comparisons among five stations in 2009 showed close agreement between the predicted AST1 and AST2 and the observed AST from AIRS, especially in the SWM season, within 1.3 K, and for *in situ* data, within 1-2 K. The validation results of both AST1 and AST2 with AST from AIRS showed high correlation coefficient (R= 0.845 - 0.918) and (R= 0.808 - 0.878), respectively, providing indication of both equations efficiency and accuracy.

Statistical analysis in term of β showed that H₂O_{vapour} (0.565–1.746) tended to contribute significantly to high AST values during the NEM season. H₂O_{vapour} (1.042–2.036) and O₃ during the SWM season were indicated by the strongly positive β (0.421-0.864). CO has a moderately positive β (0.125–0.96) associated with AST values, and CH₄ (-0.525–0.426) is also an important parameter in determining the variability of the AST value. CO₂ yields a reasonable relationship with AST by low to moderate β values (between -0.065 and 0.238).

The result of fitting the best regression equations for the O₃ data gave close to the same values of R (\approx 0.93) and R² (\approx 0.86) for both the NEM and SWM seasons.

The common variables that appeared in both equations PCA1 and PCA2 were the SSKT, CH₄ and RH, and the principal precursor of the O₃ value in both NEM and SWM seasons was SSKT. The obtained validation results between the predicted and observed O₃ showed high R (0.845–0.942) is evidence of the O₃ regression equations efficiency.

Generally, these results clearly indicate the advantage of using the satellite AIRS data and a correlation analysis study to investigate the impact of atmospheric GHGs on AST over peninsular Malaysia. Regression equations developed capable of retrieving Peninsular Malaysian AST in all weather conditions with total uncertainties ranging between 1-2 K.

CHAPTER 1

INTRODUCTION

1.0 Overview

Minute changes in the temperature of the human body can lead to sickness and even death. Similarly, the earth is highly sensitive to small changes in temperature. There is growing consensus that, since the start of the industrial revolution in the 19th century, the concentration of greenhouse gases (GHGs) in the atmosphere has increased due to continuous increases in anthropogenic emissions resulting from increased human activity, industrialisation, and deforestation. This increase in GHGs concentration has led to a rise in atmospheric and ocean temperatures, melting glaciers and ice caps, and increasing sea levels (IPCC, 2007), which have caused regional shifts in precipitation patterns and increases in the occurrence of severe weather. Natural causes alone cannot satisfactorily explain the observed warming (Gillett *et al.*, 2008).

The GHGs trap the energy from the sun and prevent heat energy from escaping back to space, thereby trapping it in the lower atmosphere, which is necessary to sustain life on earth. Global warming, the gradual decreasing in the amount of global guide irradiance at the earth's surface that was observed for several decades, and the associated changes in the world climate pattern are considered worldwide to be a serious threat to humanity in the 21th century (Lau *et al.*, 2009).

The greenhouse effect is a phenomenon created by retention of heat by the gases in the atmosphere, through absorption of the infrared light produced or reflected by the earth which warm a planet's lower atmosphere and surface, which was suggested by Joseph Fourier in 1824 and investigated quantitatively by Svante Arrhenius in 1896. This natural phenomenon is very important for life on earth

because it maintains worldwide average temperatures around 18°C; if not for the greenhouse effect, the earth would be uninhabitable (roughly -15°C) (TDOGW, 2009).

The warmest temperatures of the past century have been recorded in the past two decades, with 2005 being the hottest year followed by 1998, 2002, 2003 and 2004. The projected surface water temperature rise between 2008 and 2100 are 1.6 °C to 2.0 °C (2.9 F to 3.6 F). The evaluated surface water temperature increase through 2008 is 0.43 °C to 0.54 °C (0.77 F to 0.97 F). Over the past one hundred years, the earth has warmed by 0.8° C (1.44 F), and past thirty years, it has warmed by 0.6° C (IPCC, 2007; Swedan, 2009). It is important to consider the causes and influences of this warming to develop appropriate methods and mechanisms to reduce or decrease it.

Climate change, an important and enduring change in the statistical distribution of weather patterns over periods ranging from decades to millions of years, is now a prominent issue that has been widely discussed throughout the world. The excessive emission of global GHGs into the atmosphere is one of the major causes of climate change. The important external variables that control climate include aerosols, solar irradiance and greenhouse gases e.g. methane (CH₄), ozone (O₃), nitric acid (NO₂), water vapour (H₂O_{vapour}) and carbon dioxide (CO₂) (Lau *et al.*, 2009).

The total flux of energy entering the earth's atmosphere consists of solar radiation (99.978%), geothermal energy (0.013%) and tidal energy (0.002%). In addition, there are other negligible sources of energy, such as accretion of interplanetary dust and solar wind, the thermal radiation of space and light from distant stars. The earth reflects 30% of the incident solar energy; 20% is reflected

from clouds, 6% is reflected from the atmosphere, and 4% is reflected from the ground (including ice, land and water). The remaining 70% of the incident energy is absorbed, with 51% being absorbed by land and water and 19% being absorbed by the atmosphere and clouds (Roth, 2010). The incident energy that is absorbed will radiate again when the earth is at thermal equilibrium, with 6% radiating from the ground and 64% from the clouds and atmosphere. Although the emission of greenhouse gases and other factors, such as changes in land use, make only a minor contribution to global warming (1%) compared to the solar input, this slight modification to the energy budget is still significant and contributes to the observed increase in oceanic and atmospheric temperature (Hill, 2004; Mather, 2004).

Equilibrium is maintained as long as the quantity of GHGs in the atmosphere stays the same and as long as the energy coming from the sun is continuous (NOAA, 2010). The GHGs are emitted from both terrestrial ecosystems (forest, soils) and natural aquatic ecosystems (lakes, rivers, estuaries, wetlands) and from anthropogenic sources. They naturally have a mean warming effect of about 33°C (59°F) (Tremblay *et al.*, 2005).

In the earth's atmosphere, the dominant infrared absorbing and emitting gases, which have different influences on the greenhouse effect, are CO₂ 9-26%, H₂O_{vapor} 36-70% (not including clouds), CH₄ 4-9% and O₃ 3-7%. Clouds affect radiation differently from water vapour because it is composed of water or ice (Blais, 2005).

Southeast Asia is experiencing rapid economic growth similar to that in Northeast Asia, and it has become one of the most heavily populated regions of the world with a vibrant mixture of cultures (Lawrence, 2004). Furthermore, it is a large source of several air pollutants due to increasing anthropogenic emissions associated with biogenic emissions from large tropical forests. The greater oxidising capacity in

the tropical regions is due to a higher UV intensity, humidity, rapid development and industrialisation (Streets *et al.*, 2001).

In Malaysia, industrialisation, urbanisation and rapid traffic growth have contributed significantly to economic growth. Pockets of heavy pollution are being created by emissions from major industrial zones, increases in the number of motor vehicles and trans-boundary pollution. Furthermore, Malaysia is situated in a humid tropical zone with heavy rainfall and high temperatures (Mahmud and Kumar, 2008; Tangang *et al.*, 2007); the cloudy conditions are an obstacle to the acquisition of high-quality and high-resolution satellite data. Thus, it is better to choose a satellite with special specifications and high resolution to overcome this problem when studying the effects of the greenhouse in the tropics.

The GHGs lead to problems for the environment, especially in areas with ambient air temperature, and they also have negative impacts on health. Therefore, it is necessary to observe and accurately document not only changes in temperature but also changes in the atmosphere GHGs to assess their impact on the environment. There are many different methods for collecting data, including meteorological and trace gas measurements from ground-based instruments, data from airborne instruments (balloons and aircraft), and satellite remote sensing.

1.1 Greenhouse gases

Many GHGs occur naturally in the atmosphere, including water vapour, methane, nitrous oxide and carbon dioxide, while others are synthetic. All GHGs are minor atmospheric components, which does not reduce the seriousness of their effects. CO₂ and O₃ have elastic vibrational motions with quantum states that can be excited by collisions at energies encountered in the atmosphere. CO₂ is a linear molecule that has a significant vibrational mode in which the molecule bends with

the oxygens on the ends, moving one way, and the central carbon, moving the other. This vibration produces a dipole moment, and thus IR radiation can be absorbed by carbon dioxide (Blais, 2005).

The energy produced by collisions (between, CO₂ and radiations reflected from the earth) will immediately heat the surrounding gas. CO₂ contributes substantially to the greenhouse effect because it is easily excited by IR radiation. Water-vapour molecules have a bent shape and a permanent dipole moment (the H atom is electron-poor, and the O atom is electron-rich). Thus, IR radiation can be absorbed and emitted during rotational transitions, which can be produced by collision energy transfer. The water has multiple effects on infrared radiation, through its condensed phase and through its vapour phase, and clouds are important infrared absorbers. Other important absorbers include nitrous oxide, CH₄ and the chlorofluorocarbons (Hill, 2004).

1.1.1 Water Vapour (H₂O_{vapour})

Atmospheric water vapour is widely recognised as a key climate variable. It is the most abundant and dominant GHGs and provides key feedback for amplifying the sensitivity of the climate to external forces (John and Soden, 2007). Water vapour is a significant gaseous source of infrared opacity with an atmospheric concentration of almost 1%, and changes in its concentrations are a result of climate warming rather than a direct result of industrialisation (Held and Soden, 2000). Evaporation of water is one of the ways that the earth releases heat; water condenses as precipitation and air transfers the heat of condensation to the outer atmosphere (Swedan, 2009).

As water vapour increases in the atmosphere, more of it will ultimately also condense into clouds. Sunlight is reflected into space by low clouds, which have a

cooling effect, and the high clouds appear to enhance the greenhouse effect. The current net influence of clouds is cooling (Hill, 2004).

1.1.2 Carbon Dioxide (CO₂)

Carbon dioxide (CO₂) is the dominant anthropogenic GHGs, and it represents an important component of climate change. Carbon dioxide is thought to be responsible for more than 50% of the current global warming when all GHGs (with the exception of water vapour) are considered together (Swedan, 2009). Its concentrations have rapidly increased since the dawn of the industrial revolution due to the burning of fossil fuels and deforestation. However, only about half of the emissions have accumulated in the atmosphere, and the fate of the remaining half remains uncertain (Jasim *et al.*, 2009).

Terrestrial biomass-containing grasses and trees store almost three times more CO₂ than the atmosphere, and oceans are the greatest CO₂ sink, containing around 50 times more carbon than the atmosphere. Half the excess CO₂ generated by human activities may be absorbed by terrestrial ecosystems and the ocean, and the remainder contributes to the growing levels of this gas in the atmosphere (5.5 ± 0.5 109-tons carbon per year (Gt C/y)) (Blais, 2005; Battle *et al.*, 2000).

1.1.3 Ozone (O₃)

Ozone (O₃) is the most important index component of photochemical smog. It has been identified as one of the primary pollutants that degrade air quality, and it naturally present in our atmosphere. Because of its ability to absorb infrared radiation it considered an essential and important greenhouse gases, and its presence both at the ground level and in the earth's upper atmosphere (Freijer *et al.*, 2002). Stratospheric ozone is considered to be beneficial for humans and other life forms

because it creates a protective shield by absorbing some of the sun's biologically harmful ultraviolet (UV)-B radiation. In humans, increased exposure to UV radiation can lead to an increase in the occurrence of skin cancer, cataracts and immune-system impairment (Bian *et al.*, 2007).

At the ground level, O₃ is a harmful pollutant that causes damage to lung tissue, plants and other living systems (Morris *et al.*, 2006), and it not emitted directly into the air but is formed by the reaction of volatile organic compounds (VOCs), which are emitted from various sources, including motor vehicles and other industrial sources. The O₃ is also formed from nitrogen oxides (NO_x) (combination of NO and NO₂) in the presence of heat and sunlight. Ground-level ozone forms easily in the atmosphere, particularly in warm sunny urban areas (Morris *et al.*, 2006). Depending on the wind direction, ozone and the precursor pollutants that form ozone can also be transported hundreds of kilometres away (DOE, 2004).

1.1.4 Methane (CH₄)

Methane (CH₄) is a potent greenhouse gas, and it is second in importance only to CO₂ with a relative global warming ability that is 23 times that of CO₂ over a time horizon of 100 years. But, fortunately, its concentrations in the atmosphere are much less than CO₂. Therefore, for the same mass, CH₄ emission will have 23 times the temperature influence compared to CO₂ emission (Yashiro *et al.*, 2008). It is formed and released to the atmosphere by biological processes occurring in anaerobic environments. CH₄ is emitted from a diversity of both human-associated (anthropogenic) and natural sources. Human-associated activities include agriculture, biomass burning, fossil fuel production, waste management, and animal husbandry. Domestic ruminant animals, especially cattle and sheep, emit about 15% of all methane (Hill, 2004).

Natural sources include wetlands, oceans, non-wetland soils, gas hydrates, permafrost, termites, freshwater bodies, and other sources such as wildfires. Because they are dominated by marshes and swamps, tropical wetlands emit large amounts of CH₄ into the atmosphere compared to northern peatlands. Moreover, CH₄ emissions are significantly higher in open peatlands than in forested peatlands (Melling *et al.*, 2005).

1.1.5 Carbon Monoxide (CO)

Worldwide, anthropogenic sources produce about 50% of the carbon monoxide (CO) emissions, with the remainder coming from biomass burning and the oxidation of naturally occurring volatile hydrocarbons. CO is a product of incomplete combustion of fossil fuel and biomass, and it has an average lifetime of 2-4 months in the atmosphere (McMillan *et al.*, 2005). CO influences oxidation in the atmosphere by interacting with hydroxyl radicals (OH) and halocarbons, but it is not considered a direct greenhouse gas because it does not absorb terrestrial thermal IR and it provides a sink for 75% of the atmospheric OH (Thompson *et al.*, 1994). It is generally agreed that biomass burning accounts for about one quarter of CO emission to the atmosphere (Liu *et al.*, 2005; Houghton, 2005).

Andreae and Merlet (2001) estimated that the annual emission of CO from vegetation fires in tropical forests and savannahs is 342 Mt (1 Mt=10⁹ kg) CO per year, while the total CO emission for all non-tropical forest fires is 68 Mt CO per year. A concentration of as little as 400 ppm (0.04%) carbon monoxide in the air can be fatal (Ford *et al.*, 2001).

1.2 IPCC and Global Warming

As reported in the IPCC Fourth Assessment Report [IPCC, 2007], “Changes in the atmospheric abundance of greenhouse gases and aerosols, in solar radiation and in land surface properties alter the energy balance of the climate system□. Figure 1.1 is from the IPCC report and clearly depicts the increase of greenhouse gas emissions. As a result of human activities since 1750, the global atmospheric concentrations of CO₂, CH₄ and N₂O have increased noticeably and far exceed pre-industrial values determined from ice cores spanning many thousands of years. During the last ten years (1995–2005 averages: 1.9 ppm per year), the annual rate of increase of the CO₂ concentration has been at its highest since the recording of continuous direct atmospheric measurements began (1960–2005 averages: 1.4 ppm per year). The primary contributor to the increased atmospheric concentration of CO₂ is fossil-fuel use; changes in land use also contribute significantly, although less than fossil fuels.

Due to the burning of fossil fuels and agricultural activities, the CH₄ concentration has increased from a pre-industrial value of about 715 ppb to 1732 ppb in the early 1990s, and it was 1774 ppb in 2005. The increase in N₂O concentration is due to agriculture, and the growth rate has been approximately constant since 1980. The increasing concentrations of greenhouse gases have a positive impact on radiative forcing, which warms the climate. Radiative forcing is a measure of the effect that a factor has on the balance of outgoing and incoming energy in the earth-atmosphere system and is an index of the significance of the factor as a potential climate change mechanism. Fig. 1.2, illustrates that the global average net effect of human activities since 1750 has resulted in warming, with a radiative forcing of +1.6

[+0.6 to +2.4] W/m⁻². The carbon dioxide radiative forcing increased by 20% from 1995 to 2005.

The combined radiative forcing due to CO₂, CH₄ and N₂O from 1750 to 2005 was +2.3 W/m⁻², with uncertainty ranges at 5% and 95% of [+2.07 to +2.53] W/m⁻². Due to emissions of ozone-forming chemicals (nitrogen oxides, carbon monoxide, and hydrocarbons), the tropospheric ozone has changed, which has resulted in a slight negative forcing of -0.05 [-0.15 to +0.05] W/m⁻² in the stratosphere and a positive radiative forcing of +0.35 [+0.25 to +0.65] W/m⁻² in the troposphere. Anthropogenic contributions to aerosols together results from a cooling impact, with a net negative direct radiative forcing of -0.5 [-0.9 to -0.1] W/m⁻² and a negative indirect cloud albedo forcing of -0.7 [-1.8 to -0.3] W/m⁻².

Changes in surface albedo are estimated to cause a radiative forcing of -0.2 [-0.4 to 0.0] and +0.1 [0.0 to +0.2] W/m⁻² because of land-cover changes and deposition of black-carbon aerosols on snow. The direct radiative forcing due to changes in halocarbons is +0.34 [+0.31 to +0.37] W/m⁻². Warming of the climate system is unequivocal, as is now evidenced by numerous long-term changes that have been observed. These changes include changes in arctic temperatures and ice, ocean salinity, wind patterns and aspects of extreme weather, including droughts, widespread changes in precipitation amounts, heat waves and the intensity of tropical cyclones since the mid-20th century and their projected continuation.

The increase of global temperatures is a reaction to increasing forcing at a rate of about 0.2°C per decade over the past 30 years. Since the dawn of the industrial revolution, the global average temperature has increased about 0.7° to 1.4° F (0.4° to 0.8° C). Figure 1.3 shows the change in the global surface temperature,

global average sea level, and northern hemisphere snow cover since 1850, relative to the 30 year 1961-1990 climatological average.

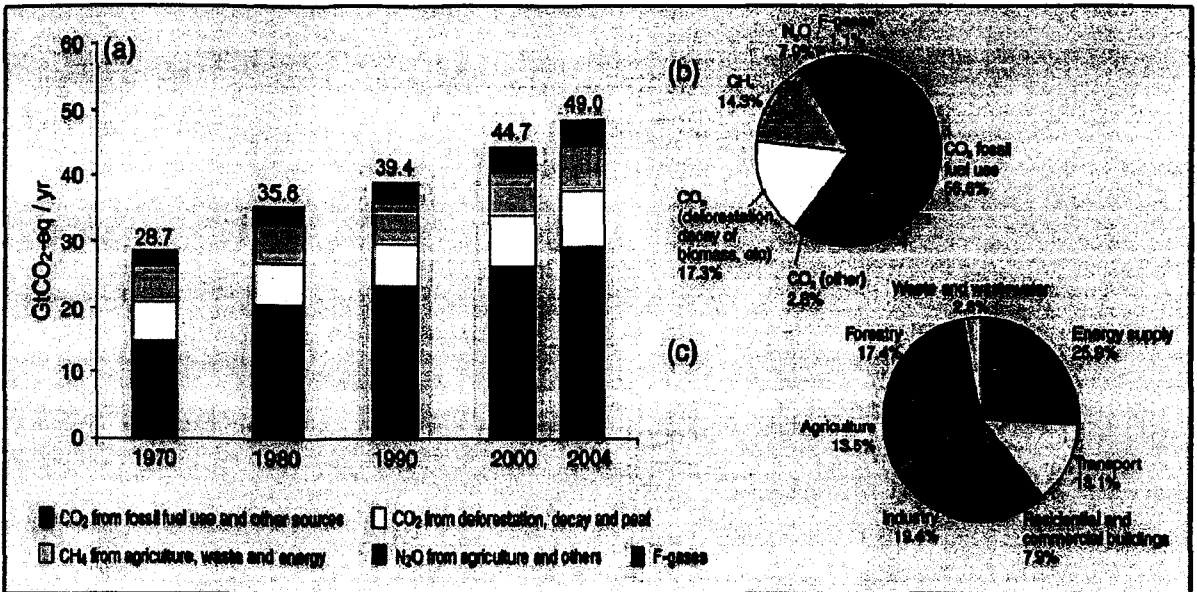


Figure 1.1: From IPCC 4th Assessment Report, (a) Global annual emissions of anthropogenic GHGs from 1970 to 2004. (b) Share of different anthropogenic GHGs in total emissions in 2004. (c) Share of different sectors in total anthropogenic GHG emissions in 2004 (IPCC, 2007).

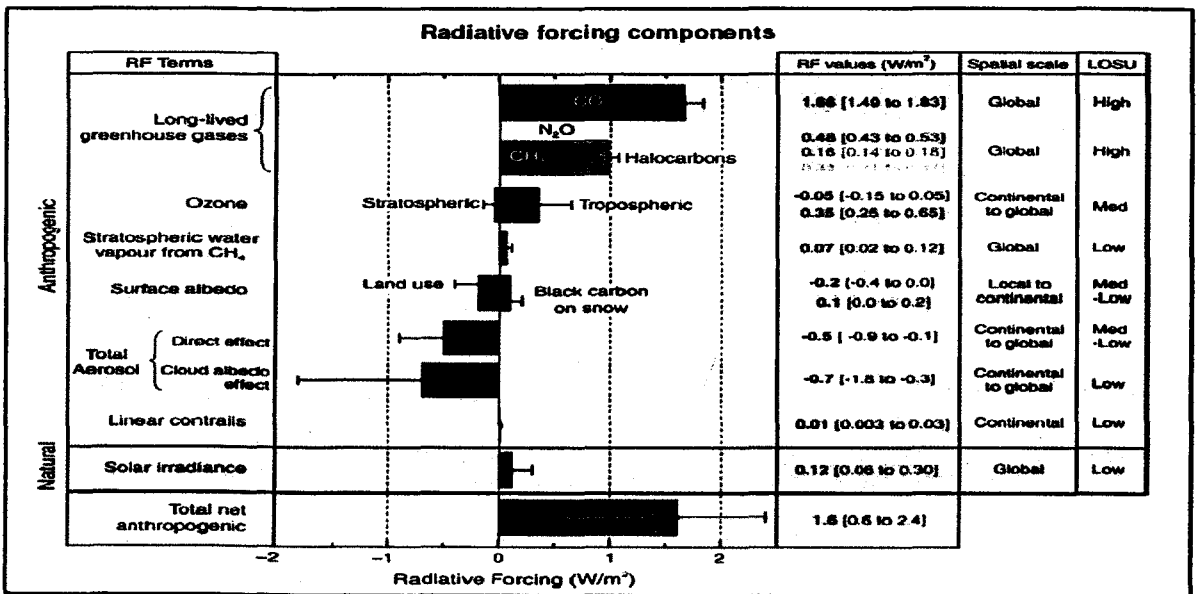


Figure 1.2: Global-average radiative forcing (RF) in 2005 (best estimates and 5-95% uncertainty ranges) with respect to 1750 for CO₂, CH₄, N₂O and other important agents and mechanisms, together with the typical geographical extent (spatial scale) of the forcing and the assessed level of scientific understanding (LOSU). Aerosols from explosive volcanic eruptions contribute an additional episodic cooling term for a few years following an eruption (IPCC, 2007).

The linear warming trend over the last 50 years is 0.13°C [0.10°C to 0.16°C] per decade, and the total temperature increase from 1850–1899 to 2001–2005 is 0.76°C [0.57°C to 0.95°C]. During the last twenty years, acceleration in the warming of the surface temperature and a decrease in snow cover has been observed. Furthermore, a consistent increase in the level of the sea has been documented since 1930.

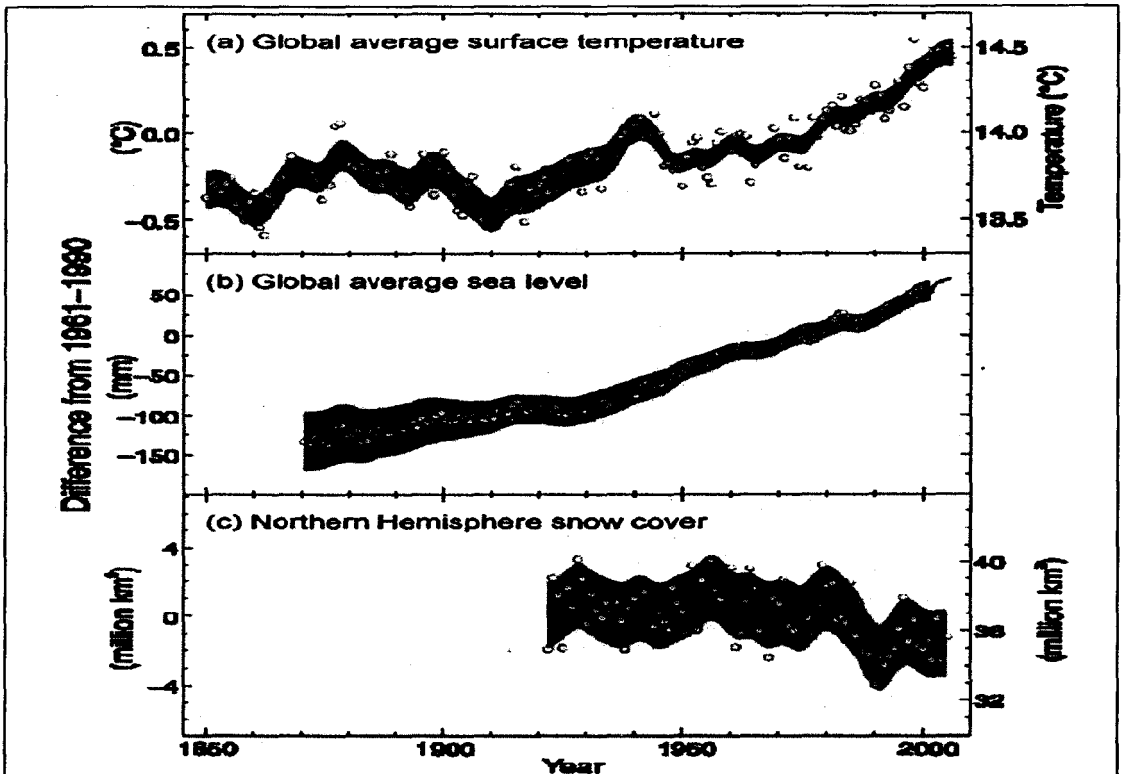


Figure 1.3: Observed changes in (a) global average surface temperature; (b) global average sea level from tide gauge (blue) and satellite (red) data and (c) Northern Hemisphere snow cover for March-April. All differences are relative to corresponding averages for the period 1961-1990. Smoothed curves represent decadal averaged values while circles show yearly values. The shaded areas are the uncertainty intervals estimated from a comprehensive analysis of known uncertainties (a and b) and from the time series (c) (IPCC, 2007).

1.3 A Definition and Brief History of Remote Sensing

The term "remote sensing" is most generally used in conjunction with electromagnetic techniques of information acquisition, which comprise the analysis

and interpretation of measurement or acquisition of information about a target without being in physical contact with it. This approach was used for observation of the earth in this study. Observation of the earth by remote sensing allows for measurements to be made by airborne or satellite instruments that detect electromagnetic radiation that is reflected or emitted by targets from the earth's surface or within the atmosphere. The goal of remote sensing is to understand the relationships between these measurements and the nature and distribution of events within the atmosphere or on the earth's surface (Mather, 2004).

The early development of remote sensing as a scientific field is closely related to developments in photography. In 1839, Daguerre and Niepce reported the first photographs. Balloons were used in 1858 to take photographs of large areas, which were followed by the use of kites in the 1880s. In the early 1900s, pigeons were used to carry cameras to many hundred metres of altitude. After the advent of the airplane, the acquisition of data over specific areas and under controlled conditions became possible, making aerial photography a very useful tool.

The first recorded aerial photographs were taken from an airplane piloted by Wilbur Wright in 1909 over Centocelli, Italy. In the mid-1930s, colour photography became available, and the field was further advanced with development of films that were sensitive to near-infrared radiation, which was particularly useful for haze penetration. Aerial photography was used for the recognition and classification of vegetation types and for the detection of damaged and diseased vegetation by Colwell in 1956.

The active microwave systems have been used since the early twentieth century, especially after World War II, to detect and track moving objects, such as ships and planes. Later, systems were developed to provide two-dimensional images.

Passive microwave sensors were also developed to generate “photographs” of the microwave emission of natural objects. The most recently introduced remote sensing instrument is the laser, which was first developed in 1960 and used for atmospheric studies, surface studies by fluorescence, and topographic mapping.

Over the past two decades, the capabilities of remote sensing satellites have dramatically increased. The number of available spectral channels has grown from a few to more than 200 in the case of the Hyperion instrument. Synthetic-aperture radars are now capable of collecting images on demand in many different modes. Satellites are now obtaining images of other planets at better resolution and with more spectral channels. Furthermore, remote sensing data have become increasingly available. In many cases, the limitation is no longer the technology but rather the techniques and training needed to optimally utilise the information embedded in the remote sensing data (Elachi and Zyl, 2006).

1.4 Remote Sensing Space Platforms

Up until 1946, remote sensing data were mainly acquired from airplanes or balloons. In 1946, sounding rocket photographs were taken from V-2 rockets, and this accomplishment proved invaluable in illustrating the potential value of photography from orbital altitudes. The systematic orbital observations of the earth started in 1960 with the launch of the first meteorological satellite, named Television Infra Red Observation Satellite (TIROS I). TIROS I was one of ten application satellites (TIROS, 1960 till 1965) using a low-resolution imaging system, and it was launched primarily to provide images of cloud formations. The second satellite had an IR camera and a five-channel radiometer that could provide both day and night cloud images.

The fourth satellite in this series was launched in February 1962 and had a low-data-rate direct broadcast capability called automatic picture transmission (APT). The first Earth Resources Technology Satellite (ERTS-1, later renamed Landsat-1) was launched in 1972, representing one of the major milestones in the field of Earth remote sensing. This satellite provided the first multispectral images that could be used to assess the value of satellite use for Earth resource observation (Coronado and Brentzel, 2006). In the late 1970s, the direct broadcast (DB), or "the real-time transmission of satellite data to the ground," was emerging.

Earth-orbiting spacecraft have also been used to acquire remote sensing data. The Nimbus spacecraft carried passive microwave radiometers, infrared spectrometers, and infrared radiometers. The visible and IR spin-scan cameras carried by the Synchronous Meteorological Satellite (SMS) and Skylab satellite (1972) carried a radiometer and a radar scatterometer. The Seasat satellite, launched in 1978, carried imaging radar, a scatterometer, and an altimeter (Elachi and Zyl, 2006). Beginning in the mid-1960s, under the sponsorship of NASA, a large number of studies investigating the use of colour infrared and multispectral photography were undertaken, leading to the launch of multispectral imagers on the Landsat satellites in the 1970s.

The Earth Observing System (EOS) program has been developed by NASA since 1980s. This program is an integrated, multi-satellite, long-term programme that will facilitate observation of the earth's land, atmosphere, and oceans as an integrated system. The EOS is providing data for in-depth scientific investigation of the functioning of the earth as a system through a constellation of satellites. Remote sensing of the earth by satellite has seen a rapid expansion during the last decade,

and it has entered a new era since the launch of the Terra and Aqua satellites in December 1999 and May 2002, respectively (Qu and Kafatos, 2006).

1.5 Problem statement

Over the past three decades, the abundances of atmospheric gases have been measured using balloons, airplanes and sparsely distributed measurement sites. The observations were mostly confined to the surface of the site. The measurements are unable to make continuous recordings of global variation over the long-term, and cost a lot of money and staff. Therefore, there is a lack of data both in the lower - particularly over land - and upper troposphere (Tiwari *et al.*, 2005).

Despite the lack, observational studies of GHGs in Malaysia, most of the studies have been carried out depending on the ground station's data, and the studies used satellite data was not considered the equatorial area. Furthermore, the climatology of Malaysia, which is one of the Southeast Asia's countries, is dominated by a strong northeast (NEM) and southwest (SWM) monsoon. These monsoons have different influences on the atmospheric parameters, in terms of the effects on climate or the amounts of pollutants; they bring to Malaysia, besides the contribution of the many regional pollutant sources. Therefore, there is a necessity to use satellite data to investigate the relationship between the atmosphere GHGs and temperature over Malaysia.

The satellite remote sensing has very good global coverage and can provide continuous data with high spatial and temporal resolution (Dousset and Gourmelon, 2003). The free download satellite AIRS data makes it the useful space instrument for observing the earth's atmospheric temperature, water vapour and the reaction of the several atmospheric GHGs with a cloud clearing system (McMillan *et al.*, 2005).

Although the AIRS provide the air surface temperatures (AST), but it is not precise as required accuracy for a small region or a certain city because the satellite data is a spot for a wide area depend on the granule's resolution. In order to better precision, it is necessary to develop a new model for calculating AST, which can use for small or any selected area.

The CO₂, CH₄, O₃ and H₂O_{vapour} are the main GHGs in the atmosphere, which contribute to warm a planet's lower atmosphere and surface through absorption of the infrared light produced or reflected by the earth. And CO is an important pervasive atmosphere trace gas affecting to the climate (McMillan *et al.*, 2005). Therefore, been the use of these gases in generating regression equations for calculating AST, and to analyse their impacts on AST values using statistical methods.

Ozone is unique among pollutants because it is not emitted directly into the air, and its results from complex chemical reactions in the atmosphere. Yet it has dramatically different effects depending on where O₃ resides, it can harm or protect life on earth (Al-Alawi *et al.*, 2008). This is the main reason why ozone is such a serious environmental problem that is difficult to predict and control. Therefore, it is necessary to generate an equation for estimating O₃ value using satellite data, and analyse the effects of the atmosphere parameters on its value. The multiple regression analysis (MRA) and principle component analysis (PCA) used in this study are the most common methodology used in the atmospheric sciences.

1.6 Objectives of the study

The objectives of the study are summarised as follows:

- 1- To develop a general regression equation for calculating the AST over peninsular Malaysia using results from the analysis of the retrieved gases in the atmosphere for the period (2003 - 2008) obtained from the AIRS data.

- 2- To estimate the ozone column (O_3) in peninsular Malaysia via the predicted regression equations using AIRS satellite data.
- 3- To investigate and analyse the influences of the GHGs (CO_2 , CH_4 , O_3 , and H_2O_{vapour}) and CO in the AST values using statistical methods.
- 4- To analyse the effects of the atmosphere parameters on O_3 values using PCA methods.

1.7 Originality

The information retrieved from the satellite retrieval has been employed to develop regression equations. The new regression equations for air surface temperature (AST) and ozone total column (O_3) has been generated, and the relationship between AST and gases is analysed using statistical methods. This work is the first study using AIRS data to develop regression equations and analyse the atmosphere parameter's effects on AST in peninsular Malaysia using statistical methods. New regression equations of AST and O_3 have been introduced and validated for 2009.

1.8 Outline of the thesis

This dissertation consists of seven chapters, which are described in brief as follows:

Chapter 1 provides an overview of this study. Additionally, this chapter presents a brief background of global warming and greenhouse gases and includes sections entitled IPCC and Global Warming, A Definition and Brief History of Remote Sensing, and Remote Sensing Space Platforms. In addition, a statement of the problem, originality, and the objectives of this study are also presented in this chapter.

Chapter 2 gives the literature overview of the related work that uses the AIRS data; it describes what is currently known about greenhouse gases and the temperature over Malaysia and statistical analysis. Chapter 3 is devoted to the detailed description of the AIRS instrument, and it describes the sources of the data and the software and tools used. For satellite data, the AIRS data were used in this study. The in situ data were obtained from the Malaysia Meteorology Department (MMD). The SPSS program was used for pre-processing and analysis tasks. The validation and comparison were done with SigmaPlot. Chapter 4 describes in detail the study area and methodology. This chapter discusses the procedure for the research and all applied techniques and methods for data processing.

Chapter 5 includes the analysis of all the obtained results and consists of four parts. The first part discusses the results of this study and the outcome of the multiple regression analysis (MRA) methods. The prediction algorithms of AST are also considered in this part of the chapter. The second part presents and discusses the results of the principal component analysis (PCA) method. In this part, the predicted algorithm of ozone is presented. The third part presents and discusses the results of the evaluation of atmosphere gases using the AIRS data for five stations. The fourth part discusses the results and describes the distribution of atmosphere gases using mapping for 2009. Chapter 6 focuses on the validation and comparisons for the two predicted algorithms, AST and O₃. Both algorithms were validated with the observed AIRS data, and compared with in-situ and observed AIRS data. Finally, the conclusions and future works are presented in Chapter 7.

CHAPTER 2

LITERATURE REVIEW

2.0 Introduction

Scientists have been tracing the world's average temperature from the late 19th century. In the late 1950s, a few scientists began to inform the public that GHGs might become a problem within the foreseeable future. Weather experts during the 1960s found that the trend had shifted to cooling over the previous couple of decades (TDOGW, 2009). Since the early 1980s, global warming and climate change have become topics of serious discussion not only within the scientific community but also among the international and the general political communities (Cheang, 1993). Many scientists believe that climate change is occurring because of an increase in the concentrations of the main GHGs, which are found naturally in the earth's atmosphere and are also emitted as a result of human activities (TDOGW, 2010).

The industrial revolution brought more extensive agriculture, new industrial processes, and a rapid increase in the world's population. Because of these increased human activities, the concentration of GHGs in the atmosphere has increased, causing a rise in temperature. The global mean temperature has increased by 0.3-0.6°C during the past 100 years, and warming has been accelerating at a rate of 0.15 since the mid-1970s. The temperature rise has adverse effects on living systems (Hopwood and Cohen, 2008).

Considering the causes and effects of the rise in temperature, so can apply the appropriate methods to evaluate the amount of GHGs in the atmosphere and evaluate their effects on temperature depending on the technique of obtaining the data and methods of analysis

For the last two decades, there has been a deficiency of studies using satellite data to explore the impacts of greenhouse gases on global warming in Southeast Asia. Most of the studies that have been carried out rely on *in situ* data and data from small areas that are close to and perturbed by regional pollution sources.

The research presented here uses the seven-year satellite data sets to develop regression equations for AST and O₃. The equations are mainly focused on the concentrations and exchange of atmospheric parameters (gases) from satellite data (AIRS). These data from AIRS are necessary and act as feedback for the contributors, who in turn can analyse the GHGs released into the atmospheric and assess the extent of their impact on the temperature. Therefore, this chapter will review the literature related to the atmospheric GHGs and surface parameters from AIRS data, GHGs and temperature over Malaysia and statistical analyses.

2.1 Greenhouse gases and temperature in Malaysia

In addition to the Malaysian Meteorology Department (MMD) data, which provides daily, monthly and annual data for atmospheric parameters and temperatures, there are many studies on global warming in Malaysia (Shahrudin and Mohamed, 2005; Tangang *et al.* 2007). Most of these studies have been conducted using ground station data. Shahrudin and Teo (2004) used surface mean maximum and minimum air temperatures from twenty-one stations throughout peninsular Malaysia as indices of climate change for a short period, 1980-1995. The results show that the trend in the diurnal temperature range (DTR) was positively correlated for urban centres in the East Coast region and highly negatively correlated in the West Coast region in all seasons.

A trend (1961–2003) in daily maximum and minimum temperatures has been documented across the Asia–Pacific region. Significant increases in maximum and

unlogged sites. The authors show that logging practices increased the soil N₂O emission and decreased the soil CH₄ absorption, and these can accelerate global warming.

Lau *et al.* (2009) compared the effective energy policies and implementation strategies in Japan and Malaysia as these nations move towards achieving their obligations to reduce the GHGs emissions and achieve the targets in the Kyoto Protocol. Malaysia has been strongly promoting several projects and policies that can substantially reduce the GHGs emission. Recommendations on how developing nations such as Malaysia could adopt the policies have been adapted in Japan to suit local conditions, and they have contributed significantly to GHG reduction.

2.2 Atmospheric composition—minor gases from AIRS

AIRS, together with the AMSU and HSB microwave radiometers, has achieved a global retrieval accuracy of better than 1 K in the lower troposphere under clear and partly cloudy conditions (Aumann, *et al.*, 2003 a). Therefore, to provide new insights into weather, climate, high-vertical resolution profiles of temperature and water vapour, and spectral features of several trace gases, the retrieved AIRS data have been used in many studies as a valuable tool to enhance the understanding of weather forecasting and to provide new data on GHGs at a low cost (Chahine, *et al.*, 2006).

Marshall, *et al.* (2006), Pagano, *et al.* (2006), Chahine, *et al.* (2008) used AIRS data to improve weather prediction and parameterisation of climate models. Furthermore, they have provided new essential information for climate study on several of the GHGs.

Aumann and Strow (2003 b) compared AIRS measurements of the sea surface temperature (SST) at 2616 cm⁻¹ against global real-time SST. They

concluded that the satellite zenith angle (sza)-independent component is strongly temperature dependent above 300 K. The sza-dependent component of about 0.4 K is most probably due to some form of marine aerosol, which is not included in the radiative transfer.

The stratospheric temperature perturbations for the gravity wave derived from the new data set near Darwin, Australia in January 2003 are compared with results from Level-2 AIRS data and compatible measurements of the High Resolution Dynamics Limb Sounder (HIRDLS). For the vertical wavelength below 10 km, the new retrieval does not show a response to wave perturbations, and the amplitudes are damped by a factor of two for 15 km vertical wavelength. The AIRS has the advantage of providing horizontal phase information and also shows a very similar wave structure to HIRDLS for the vertical wavelengths greater than 20 km (Hoffmann and Alexander, 2009).

Aumann *et al.* (2006) analysed the difference between the brightness temperature calculated at the top of the atmosphere (TOA) and those measured at 2616 cm^{-1} using the Real Global Sea Surface Temperature (RTGSST) for cloud-free night tropical oceans between $\pm 30^\circ$ to evaluate the stability and absolute accuracy of radiometric calibration of the AIRS. The analysis achieved absolute calibration at 2616 cm^{-1} to be better than 200 mK with better than 16 mK/yr stability for the first three years of AIRS radiances.

AIRS Level-3, version 5 daily descending (night-time) and ascending (daytime) temperature profile data were used to identify the inversion effects on nitrogen dioxide (NO_2) and fine particulate matter ($\text{PM}_{2.5}$) in the atmosphere over Ontario, Canada for the period from 2003-2007. The results show daytime inversion effects corresponding to an 11% increase for NO_2 and a 14% decrease for $\text{PM}_{2.5}$.